

- 0.9 ( $\pm 0.4$ ); 153 to 155, 1.3 ( $\pm 0.5$ ); 163 to 164, 1.6 ( $-0.7$ ,  $+0.9$ ); 167 to 170, 2.0 ( $-0.6$ ,  $+0.8$ ); 174 to 175, 2.7 ( $-1.3$ ,  $+1.8$ ); 180 to 181, 1.8 ( $\pm 0.6$ ); 183 to 189, 0.9 ( $\pm 0.3$ ); 200 to 203, 1.0 ( $-0.4$ ,  $+0.6$ ); 204 to 208, 0.3 ( $\pm 0.1$ ); 212 to 215, 0.9 ( $\pm 0.5$ ); 220 to 222, 0.03; 263 to 268, 0.05; 272 to 276, 0.06; 280 to 283, 0.1 ( $-0.2$ ,  $+0.3$ ); 300 to 306, 0.03; 327 to 331, 0.02 ( $-0.006$ ,  $+0.02$ ); and 342 to 347, 0.3 ( $-0.1$ ,  $+0.2$ ).
22. A sequence-independent decrease in the extent of cleavage after the addition of  $Mg^{2+}$  was observed within the dead time of the experiment (20 ms). Because a similar result was obtained with 0.5 to 1.0 M KCl, we attribute this decrease to either a general electrostatic effect on ribose oxidation or a decrease in the steady-state concentration of hydroxyl radical, rather than to any specific folding transition in the RNA. However, it is possible that monovalent cations induce a conformational change within the first 20 ms (28).
  23. F. L. Murphy and T. R. Cech, *J. Mol. Biol.* **236**, 49 (1994).
  24. J. H. Cate, R. L. Hanna, J. A. Doudna, *Nature Struct. Biol.* **4**, 553 (1997).
  25. B. Laggerbauer, F. L. Murphy, T. R. Cech, *EMBO J.* **13**, 2699 (1994).
  26. E. A. Doherty and J. A. Doudna, *Biochemistry* **36**, 3159 (1997).
  27. V. Lehnert, L. Jaeger, F. Michel, E. Westhof, *Chem. Biol.* **3**, 993 (1996).
  28. P. E. Cole, S. K. Yang, D. M. Crothers, *Biochemistry* **11**, 4358 (1972).
  29. S. L. Brehm and T. R. Cech, *ibid.* **22**, 2390 (1983).
  30. B. Sclavi, S. A. Woodson, M. Sullivan, M. R. Chance, M. Brenowitz, *Methods Enzymol.*, in press.
  31. Supported by grants from NIH (GM39929, GM51506, and GM52348), the Molecular Biophysics Training Program (GM08572), NSF (MCB-9410748 and MCB-9601148), and the Hirschl Weill-Caulier Trust. S.W. acknowledges the Pew Scholars Program and the Henry and Camille Dreyfus Foundation. The construction and operation of beamline X-9A are supported by the National Center for Research Resources, Biomedical Technology Program (P41-RR01633). The NLS is supported by the Department of Energy, Division of Materials Sciences. The data in this paper are from a thesis to be submitted by B.S. in partial fulfillment of the requirements for the degree of Doctor of Philosophy in the Sue Golding Graduate Division of Medical Sciences, Albert Einstein College of Medicine.

20 August 1997; accepted 14 January 1998

## Kinetic Intermediates Trapped by Native Interactions in RNA Folding

Daniel K. Treiber, Martha S. Rook, Patrick P. Zarrinkar,\*  
James R. Williamson†

In the magnesium ion-dependent folding of the *Tetrahymena* ribozyme, a kinetic intermediate accumulates in which the P4-P6 domain is formed, but the P3-P7 domain is not. The kinetic barriers to P3-P7 formation were investigated with the use of in vitro selection to identify mutant RNA molecules in which the folding rate of the P3-P7 domain was increased. The critical mutations disrupt native tertiary interactions within the P4-P6 domain and increase the rate of P3-P7 formation by destabilizing a kinetically trapped intermediate. Hence, kinetic traps stabilized by native interactions, and not simply by mispaired nonnative structures, can present a substantial barrier to RNA folding.

RNA forms complex structures that are able to perform a variety of functions ranging from ligand binding to catalysis. However, the mechanism by which an RNA molecule folds into a unique three-dimensional structure remains poorly understood. To study the  $Mg^{2+}$ -dependent kinetic folding pathways of large, highly structured RNA molecules such as the *Tetrahymena* ribozyme and ribonuclease (RNase) P, we have previously developed a kinetic oligonucleotide hybridization assay (1, 2). This assay exploits the selective accessibility of unfolded RNAs to sequence-specific oligodeoxynucleotide probes, the binding of which confers sensitivity to cleavage by RNase H. Folding is initiated by the addition of  $Mg^{2+}$ , and the fraction of unfolded RNA at various times is scored in a cleavage reaction containing DNA probes and RNase H. On addition of  $Mg^{2+}$  to the

*Tetrahymena* ribozyme, the two structural domains that constitute the catalytic core—P4-P6 [base-paired (P) regions 4 to 6, positions 104 to 261] and P3-P7 (P3, P7, and P8)—form sequentially as kinetic folding units (1, 3). Formation of P4-P6 is rapid ( $60 \text{ min}^{-1}$ ) (4), whereas P3-P7 forms slowly, on the minute time scale (1). This order of kinetic folding events is supported by chemical modification (5), ultraviolet cross-linking (6), and x-ray footprint (4) analysis. In the proposed folding pathway (1, 3), an intermediate ( $I_2$ ) accumulates in which only P4-P6 is folded, and the rate-limiting step for P3-P7 formation is the unimolecular rearrangement of  $I_2$  to intermediate  $I_3$ . Slow unimolecular folding steps have also been identified for the group I intron b15 (7) and RNase P (2), and they may be a general feature in the folding of large RNAs.

Mutations that increase the rate of folding of proteins have provided insight into the mechanism of slow folding steps (8). We developed an in vitro selection scheme to identify mutant *Tetrahymena* ribozymes in which the slow P3-P7 folding step ( $I_2 \rightarrow I_3$ ) is accelerated (9). Ribozymes that fold rapidly after  $Mg^{2+}$  addition were selected from a pool of RNAs containing an average of four mutations per molecule. Slow-fold-

ing RNAs were selectively depleted from the pool by kinetic oligonucleotide hybridization with probes targeting P3 and P7. A step was included in each cycle of selection to ensure that fast folding mutants formed an intact catalytic core (9). After nine rounds, the folding rate of the pool ( $G_9$ ) had increased by a factor of 4 relative to that of the initial pool ( $G_0$ ) and by a factor of 2 relative to that of the wild type (Fig. 1). Twenty-four individual molecules were cloned from the  $G_9$  pool, and the folding rate of the P3-P7 domain for five of these clones was at least three to five times that of the wild type at  $37^\circ\text{C}$  (Fig. 1 and Table 1) (10, 11).

Because each fast folding clone contained at least three mutations, individual point mutants were constructed. For the four clones analyzed, a single mutation was sufficient to reproduce the fast folding phenotype (Table 1). The A183U (A at posi-

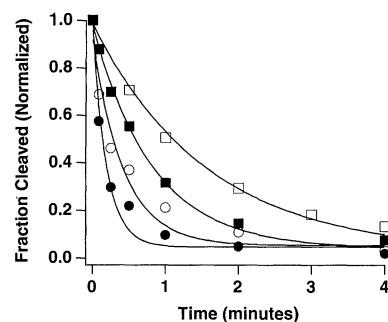


**Fig. 1.** Isolation of fast folding RNAs after nine rounds of in vitro selection. The kinetics of P3-P7 formation for ribozyme generations  $G_0$  to  $G_9$  and cloned individual molecules from  $G_9$  were probed by kinetic oligonucleotide hybridization. Initiation of folding and the quench reaction were as described (9). The fraction cleaved at each folding time was determined by denaturing PAGE and Phosphorimager analysis (Molecular Dynamics). The apparent folding rate constant ( $k_{\text{fold}}$ ) was calculated by fitting curves to a single exponential (10). Data were normalized to allow direct comparison. RNAs and  $k_{\text{fold}}$  values: □,  $G_0$  pool ( $0.63 \text{ min}^{-1}$ ), ■, wild type ( $1.2 \text{ min}^{-1}$ ), ○,  $G_9$  pool ( $2.33 \text{ min}^{-1}$ ), and ●, clone  $G_9$ -10 ( $5.0 \text{ min}^{-1}$ ).

D. K. Treiber and J. R. Williamson, Department of Molecular Biology, MB33, Scripps Research Institute, 10550 North Torrey Pines Road, La Jolla, CA 92037, USA.

M. S. Rook and P. P. Zarrinkar, Department of Chemistry, Massachusetts Institute of Technology, Cambridge, MA 02139, USA.

\*Present address: Center for Cellular and Genetic Therapies, Department of Surgery, Duke University Medical Center, Durham, NC 27710, USA.

†To whom correspondence should be addressed.

tion 183 → U), A171G, U167C, and +G174 (G insertion at position 174) mutations are all localized in the P5abc region of the P4-P6 domain (Fig. 2A), suggesting a common mechanism of action. The mutations did not greatly affect either catalysis

or the stability of P3-P7 (Table 1). Thus, although P5abc makes no direct contacts with P3-P7 in the three-dimensional structure model (12) and the P4-P6 domain acquires its native structure before P3-P7 formation (4), positions in P5abc affect the folding rate of P3-P7.

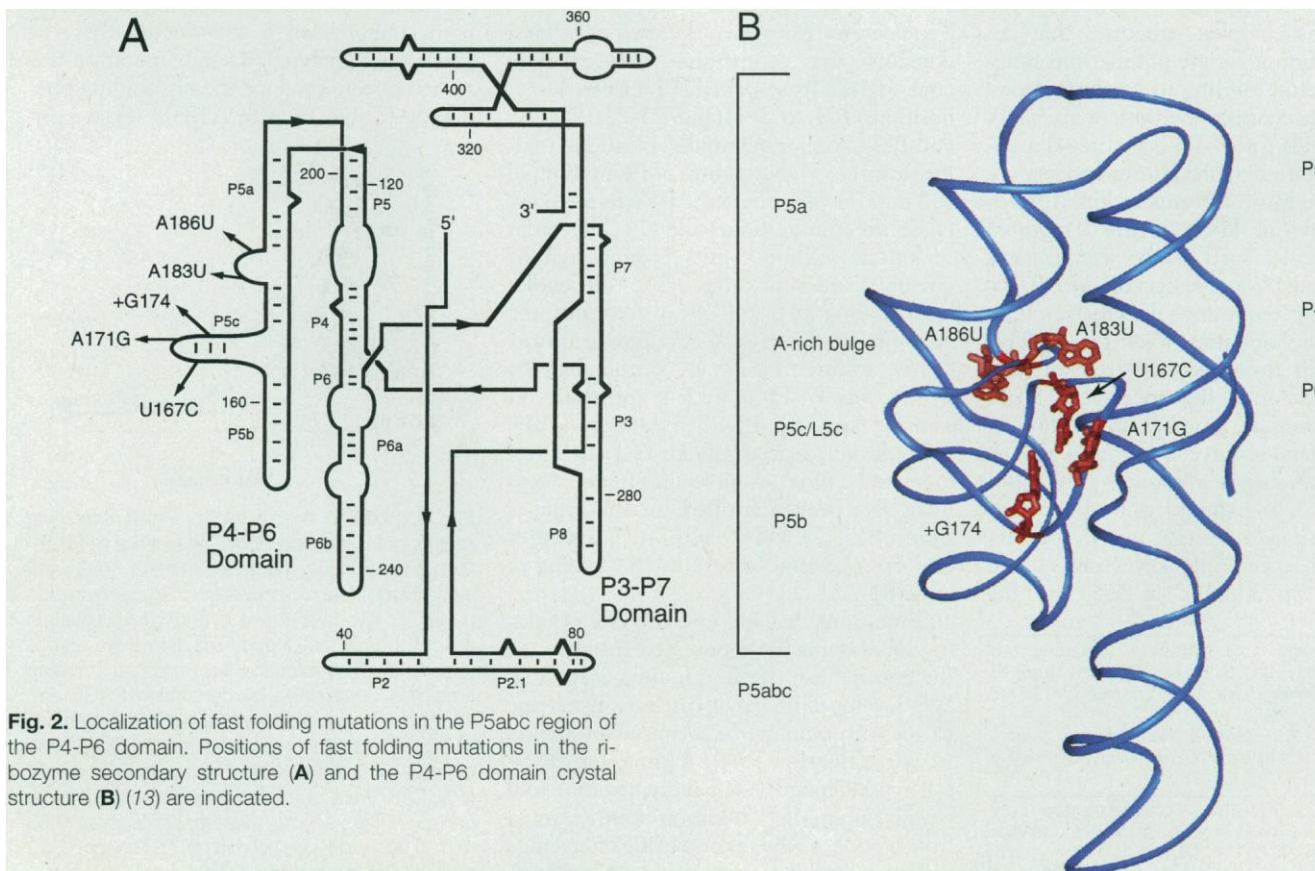
**Table 1.** Kinetic and thermodynamic constants for the folding and activity of fast folding mutants. P3-P7 folding kinetics for the clones and corresponding point mutants (second and fourth columns, respectively) were measured as in Fig. 1. Mutations that did not affect folding are not listed. The precision of the  $k_{\text{fold}}$  values was generally a factor of ~1.5. The stability of P3-P7 for each point mutant ( $[\text{Mg}^{2+}]_{1/2}$ ) was measured by  $\text{Mg}^{2+}$  titration as described (7). RNA molecules were equilibrated for 25 min at 37°C in 0.2 to 10.0 mM  $\text{MgCl}_2$ . At each  $\text{Mg}^{2+}$  concentration, the fraction of molecules folded was determined by oligonucleotide hybridization targeting P3.  $[\text{Mg}^{2+}]_{1/2}$ , the concentration of  $\text{Mg}^{2+}$  required for half-maximal folding, was calculated by fitting curves to the Hill equation. For each point mutant, the integrity of the catalytic core was assessed by measuring the rate constant for the chemical step ( $k_c$ ) in a single-turnover cleavage reaction as described (3). Ribozyme (50 to 100 nM) was annealed in TE buffer and allowed to fold for 10 min at 37°C in  $k_c$  buffer [50 mM MES (pH 5.5), 10 mM  $\text{MgCl}_2$ , 10 mM NaCl, and 1 mM dithiothreitol]. The reaction was initiated by adding 5'  $^{32}\text{P}$ -labeled substrate (CCCUC-UAAAAA) and guanosine triphosphate (final concentrations, 0.5 nM and 0.5 to 2.0 mM, respectively) in  $k_c$  buffer. The fraction of molecules cleaved at various times was determined by denaturing PAGE, and  $k_c$  was calculated by fitting curves to a single exponential.  $k_c$  values were constant ( $\pm 0.02 \text{ min}^{-1}$ ) in the range of ribozyme and guanosine triphosphate concentrations tested, confirming that the conditions were saturating. The fraction of active molecules was similar for wild-type and mutant ribozymes (28).

Clone	P3-P7 $k_{\text{fold}}$ ( $\text{min}^{-1}$ )	Mutation	P3-P7 $k_{\text{fold}}$ ( $\text{min}^{-1}$ )	$[\text{Mg}^{2+}]_{1/2}$ (mM)	$k_c$ ( $\text{min}^{-1}$ )
Wild type	1.2		1.2	1.0	0.20
A186U	4.7*	A186U	4.7*	<2†	ND‡
G <sub>9</sub> -10	5.0	A183U	5.0	1.4	0.19
G <sub>9</sub> -18	5.0	A171G	4.6	1.2	0.16
		U167C	4.5	1.2	0.13
G <sub>9</sub> -22	4.0	U167C	4.5	1.2	0.13
G <sub>9</sub> -24	6.0	+G174§	4.5	1.4	0.18

\*For A186U, P3 and P7 folding kinetics were measured separately. The value listed is the average of these measurements, which were almost identical. Separate measurements for the other mutants were also similar. †Estimated in (16) with hydroxyl radical protection assays. ‡ND, not determined. §Insertion of G at position 174.

The P5abc mutations are clustered throughout the “magnesium core” of P4-P6 in the domain crystal structure (Fig. 2B) (13). Single-atom changes that disrupt the  $\text{Mg}^{2+}$  binding sites destabilize the entire P4-P6 domain (13). Given that all of the fast folding mutations are likely to disrupt the highly cooperative network of interactions within the core, destabilization of P4-P6 in  $I_2$  may increase the rate of P3-P7 formation. The potentially destabilizing effects of the A171G and A183U mutations are especially apparent. A171 is within an adenosine platform motif in the loop of P5c (L5c) (13) that may stabilize P5c or mediate pairing between L5c and the P2 loop in the proposed P14 helix (12, 14). Furthermore, the R<sub>p</sub> phosphate oxygen of A171 directly coordinates  $\text{Mg}^{2+}$  (13). The A183U mutation disrupts two hydrogen bonds that directly bridge the helical stacks in P4-P6 (13).

If the fast folding mutations destabilize P4-P6, then other destabilizing mutations such as A186U (15, 16) should also accelerate folding. A186U disrupts five hydrogen



bonds with three different nucleotides in the three-way junction (13) (Fig. 2). This mutation accelerates P3-P7 formation by the same factor as that observed for the selected mutations (Table 1), suggesting that destabilization of P4-P6 in  $I_2$  is the common mechanism of action (17).

Given that destabilization of native P4-P6 interactions increases the rate of P3-P7 formation, we propose that  $I_2$  is a kinetic trap. In protein and RNA folding, the hallmark of a kinetic trap is that the folding rate is increased in the presence of a denaturant. Although denaturants typically reduce the rate of protein folding, they can also increase the rate of protein (18) and RNA (19) folding by destabilizing kinetically trapped intermediates. Urea markedly increased the rate of P3-P7 formation in the wild-type ribozyme (Fig. 3) but had a much smaller effect on the folding rate of the A183U mutant. Hence, a kinetic trap that is present in the folding of the wild-type ribozyme is diminished by the A183U mutation (20).

Kinetic traps in both RNA and protein folding are often misfolded structures that slow folding because stable nonnative interactions must be disrupted to achieve the transition state. Incorrect heme coordination in cytochrome c (21) and mispairing in tRNA (22) are examples of nonnative interactions that must be disrupted for folding to proceed. However, in the folding of bovine pancreatic trypsin inhibitor, a trapped intermediate is stabilized solely by native interactions (18). Furthermore, in the major folding pathway of lysozyme, an intermediate with a folded  $\alpha$  domain slows folding of the  $\beta$  domain (23). It has been suggested that the lysozyme intermediate is a kinetic trap in which the stability of a native  $\alpha$  domain renders the polypeptide rigid and "aggravates" the conformational search of the  $\beta$  domain (24). We propose a similar mecha-

nism to explain the slow folding of P3-P7.

The kinetic trap ( $I_2$ ) in ribozyme folding exhibits both native (P4-P6) and nonnative (P3-P7) structures and may also exhibit nonnative interactions at the domain interface (6). Each of these structural features might restrict the conformational flexibility of  $I_2$  and slow P3-P7 formation. However, because mutations that destabilize P4-P6 diminish the kinetic trap, the contribution of the nonnative structures to the stability of the trap is either minimal or strictly dependent on the presence of a stable P4-P6 domain.  $I_2$  is thus a native kinetic trap because its stability is derived primarily from native interactions.

The proposed native kinetic trap differs fundamentally from the canonical mispairing traps observed in tRNA (22) and ribozymes (25) and may define a new class of barriers in the folding of multidomain RNAs. Furthermore, our data show that stable intermediates are prevalent but non-essential features of RNA folding and that destabilization of an intermediate accelerates folding by facilitating escape from a native kinetic trap. These conclusions support theoretical folding models and emphasize the parallels between protein and RNA folding (3, 26).

## REFERENCES AND NOTES

- P. P. Zarrinkar and J. R. Williamson, *Science* **265**, 918 (1994).
- P. P. Zarrinkar, J. Wang, J. R. Williamson, *RNA* **2**, 564 (1996).
- P. P. Zarrinkar and J. R. Williamson, *Nature Struct. Biol.* **3**, 432 (1996).
- B. Sclavi, M. Sullivan, M. R. Chance, M. Brenowitz, S. A. Woodson, *Science* **279**, 1940 (1998); B. Sclavi, S. Woodson, M. Sullivan, M. R. Chance, M. Brenowitz, *J. Mol. Biol.* **266**, 144 (1997).
- A. R. Banerjee and D. H. Turner, *Biochemistry* **34**, 6504 (1995).
- W. D. Downs and T. R. Cech, *RNA* **2**, 718 (1996).
- K. M. Weeks and T. R. Cech, *Science* **271**, 345 (1996).
- C. D. Waldburger, T. Jonsson, R. T. Sauer, *Proc. Natl. Acad. Sci. U.S.A.* **93**, 2629 (1996); M. Munson, K. S. Anderson, L. Regan, *Folding Design* **2**, 77 (1997); D. M. Rothwarf and H. A. Scheraga, *Biochemistry* **35**, 13797 (1996).
- A four-step cycle was used to select fast folding RNAs. **Step 1:** Pools of radiolabeled ribozymes terminating at position G414 were transcribed with T7 RNA polymerase from 2 pmol of template DNA in reaction mixtures containing [ $\alpha$ - $^{32}$ P]adenosine triphosphate. Twenty picomoles of RNA was always transferred to step 2. For round one, a template DNA pool with ~1% degeneracy was created by mutagenic polymerase chain reaction [R. C. Cadwell and G. F. Joyce, *PCR Methods Applic.* **2**, 28 (1992)]. **Step 2:** Catalytically active and inactive mutants were distinguished in a ligation reaction as described [A. A. Beaudry and G. F. Joyce, *Science* **257**, 635 (1992)]. Active ribozymes cleave substrate RNA [GGCCUUA<sub>3</sub>(UA)<sub>3</sub>] to produce a ribozyme product with the 3' substrate sequence (boldface) ligated to G414. RNA pools (0.4  $\mu$ M ribozyme) were reacted with substrate RNA (3.0  $\mu$ M) for 10 min at 50°C in a solution containing 30 mM *N*-[2-hydroxyethyl]piperazine-*N'*-[3-propanesulfonic acid] (pH 7.5) and 10 mM MgCl<sub>2</sub>. **Step 3:** For selection of mutants with fast folding P3-P7 domains, ribozymes from step 2 were annealed in TE buffer [10 mM tris (pH 8.0) and 1 mM EDTA (disodium salt)] by heating at 95°C for 1 min, followed by equilibration at 37°C for 3 min. Folding was initiated by adding an equal volume of 2 $\times$  folding buffer [1 $\times$ : 50 mM tris (pH 8.0), 10 mM MgCl<sub>2</sub>, 10 mM NaCl, 0.1 mM EDTA (disodium salt), and 1 mM dithiothreitol]. After 5 s at 37°C, RNAs with unfolded P3-P7 domains were cleaved selectively by incubation (30 s at 37°C) with oligonucleotide probes (60  $\mu$ M) complementary to the 3' strands of P3 (positions 268 to 281) and P7 (positions 303 to 316) and RNase H (U.S. Biochemical; final concentration, 0.1 U/ $\mu$ l) in 1 $\times$  folding buffer. Full-length RNAs were purified by denaturing polyacrylamide gel electrophoresis (PAGE). This treatment results in the cleavage of >85% of wild-type RNA. Both P3 and P7 probes were included to reduce the likelihood of selecting mutants that were simply mismatched with the probes. **Step 4:** Catalytically active RNAs that were not cleaved in step 3 were selectively copied by priming cDNA synthesis with an oligonucleotide complementary to the ligated substrate RNA. RNA from step 3 was incubated for 45 min at 37°C with 0.33  $\mu$ M primer, 0.5 mM deoxynucleoside triphosphates, and murine leukemia virus reverse transcriptase (10 U/ $\mu$ l) (U.S. Biochemical) in the supplied buffer. The resulting cDNA was amplified by the polymerase chain reaction with Taq polymerase (Perkin-Elmer).
- The fast folding pool ( $G_3$ ) and cloned individual molecules from the pool exhibited various degrees of biphasic folding kinetics. The fast phase generally accounted for 75 to 90% of the folding amplitude. Because the slow phase was minimal, single-exponential curve fitting provided a useful means for comparison; however, the rates for the fast and slow phases are likely to be underestimated and overestimated, respectively. Biphasic folding of cloned individual RNAs suggests that more than one pathway may lead to the folded state.
- In general, the activation energy for P3-P7 formation is substantially lower for the fast folding mutants than for the wild type. Thus, at temperatures below 37°C, the rate of P3-P7 formation in some mutants is one to two orders of magnitude faster than that in the wild type (27).
- V. Lehnert, L. Jaeger, F. Michel, E. Westhof, *Chem. Biol.* **3**, 993 (1996).
- J. H. Cate *et al.*, *Science* **273**, 1678 (1996); J. H. Cate *et al.*, *ibid.*, p. 1696; J. H. Cate, R. L. Hanna, J. A. Doudna, *Nature Struct. Biol.* **4**, 553 (1997).
- The observation that A171G disrupts the adenosine platform suggests that destabilization of P14 also may increase the rate of P3-P7 formation. A second P14 mutation (G44A) acts synergistically with a distant mutation to accelerate P3-P7 formation (D. K. Treiber and J. R. Williamson, unpublished data). Because G44 is in the P2 loop, far removed from P5abc, it is likely that the stability of P14 influences the rate of P3-P7 formation. This observation also raises the possibility that P14 is formed in  $I_2$ .
- F. L. Murphy and T. R. Cech, *Biochemistry* **32**, 5291 (1993); *J. Mol. Biol.* **236**, 49 (1994).
- B. Lagerbauer, F. L. Murphy, T. R. Cech, *EMBO J.* **13**, 2669 (1994).
- Mutations that destabilize  $I_2$  are not necessarily expected to destabilize structure in the folded molecule. For example, A186U markedly destabilizes the isolated P4-P6 domain, which, in some ways, may resemble  $I_2$  (15), but it has little effect on the stability of the full-length ribozyme (16). These results are consistent with our observation that the fast folding mutations have little effect on the stability of the folded structure (Table 1).
- J. S. Weissman and P. S. Kim, *Science* **253**, 1386 (1991).
- J. Pan, D. Thirumalai, S. A. Woodson, *J. Mol. Biol.* **273**, 7 (1997); T. Pan and T. R. Sosnick, *Nature Struct. Biol.* **4**, 931 (1997).
- Urea has little or no effect on the folding rates of the +G174, U167C, and A171G mutants, suggesting that these mutations also diminish the kinetic trap (27).
- T. R. Sosnick, L. Mayne, R. Hiller, S. W. Englander, *Nature Struct. Biol.* **1**, 149 (1994).
- P. E. Cole, S. K. Yang, D. M. Crothers, *Biochemistry* **11**, 4358 (1972).
- S. E. Radford, C. M. Dobson, P. A. Evans, *Nature*

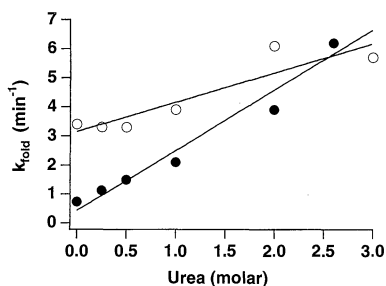


**Fig. 3.** Destabilization of a kinetic trap by fast folding mutations. The kinetics of P3 formation for wild-type (●) and A183U (○) ribozymes were measured in the presence of various concentrations of urea. RNAs were folded as in Fig. 1, with the exception that 2 $\times$  folding buffer also contained urea. Folding was quenched with RNase H and oligonucleotides targeting P3 (positions 270 to 279).

- 358, 302 (1992); A. Miranker, C. V. Robinson, S. E. Radford, R. T. Aplin, C. M. Dobson, *Science* **262**, 896 (1993).
24. G. Wildegger and T. Kiefhaber, *J. Mol. Biol.* **270**, 294 (1997).
25. S. A. Woodson and T. R. Cech, *Biochemistry* **30**, 2042 (1991).
26. D. E. Draper, *Trends Biochem. Sci.* **21**, 145 (1996); D. Thirumalai and S. A. Woodson, *Accounts Chem. Res.* **29**, 433 (1996); K. A. Dill and S. Chan, *Nature Struct. Biol.* **4**, 10 (1997).
27. M. S. Rook, D. K. Treiber, J. R. Williamson, in preparation.
28. For each mutant, the fraction of active molecules at 37°C was determined by measuring the kinetic burst in a multiple-turnover cleavage assay as described [D. Herschlag and T. R. Cech, *Biochemistry* **29**, 10159 (1990)]. In all instances, the active ribozyme concentration was nearly equal to the total ribozyme concentration. This result was obtained whether the ribozymes were prefolded in either 10 or 2 mM Mg<sup>2+</sup>, indicating that the mutations do not markedly destabilize the final, active conformation.
29. We thank P. Kim and B. Tidor for reviewing the manuscript, J. W. Orr for assistance with Fig. 2, and T. R. Cech for providing A186U plasmid DNA. Supported by the Rita Allen Foundation, the Alfred P. Sloan Foundation, and the Camille and Henry Dreyfus Foundation (J.R.W.). D.K.T. was supported by an American Cancer Society postdoctoral fellowship and P.P.Z. by a Howard Hughes Medical Institute predoctoral fellowship.

29 August 1997; accepted 4 February 1998

## Energy Transduction on the Nanosecond Time Scale: Early Structural Events in a Xanthopsin Photocycle

Benjamin Perman, Vukica Šrajer, Zhong Ren, Tsu-yi Teng, Claude Pradervand, Thomas Ursby, Dominique Bourgeois, Friederich Schotte, Michael Wulff, Remco Kort, Klaas Hellingwerf, Keith Moffat\*

Photoactive yellow protein (PYP) is a member of the xanthopsin family of eubacterial blue-light photoreceptors. On absorption of light, PYP enters a photocycle that ultimately transduces the energy contained in a light signal into an altered biological response. Nanosecond time-resolved x-ray crystallography was used to determine the structure of the short-lived, red-shifted, intermediate state denoted [pR], which develops within 1 nanosecond after photoelectronic excitation of the chromophore of PYP by absorption of light. The resulting structural model demonstrates that the [pR] state possesses the *cis* conformation of the 4-hydroxyl cinnamic thioester chromophore, and that the process of *trans* to *cis* isomerization is accompanied by the specific formation of new hydrogen bonds that replace those broken upon excitation of the chromophore. Regions of flexibility that compose the chromophore-binding pocket serve to lower the activation energy barrier between the dark state, denoted pG, and [pR], and help initiate entrance into the photocycle. Direct structural evidence is provided for the initial processes of transduction of light energy, which ultimately translate into a physiological signal.

mophore is completely buried with no atom exposed to solvent (6). These properties contribute to the protein's characteristic absorption peak at a wavelength of 446 nm (4, 7, 8). Upon photoelectronic excitation, PYP efficiently enters a fully reversible photocycle that contains at least two spectrally distinct intermediate states, denoted [pR] and [pB], each presumably associated with structural changes in the chromophore and its protein environment (Fig. 1). The rate constants for interconversion of the intermediate states progressively decrease throughout the photocycle (7), and therefore, the presumed signaling state [pB] accumulates under constant illumination that populates a saturated photostationary state (9). Time-resolved x-ray crystallographic studies with 10-ms time resolution of the decay from this photostationary state confirm that the chromophore is in the *cis* conformation (10) as predicted by chemical studies (11). The decay was shown to involve ejection of the chromophore from its binding pocket, displacement of the side chain of Arg<sup>52</sup> that closes the chromophore-binding pocket, exposure of the chromophore to the solvent, its protonation (10, 12), and concomitant major rearrangement of the H-bond network that stabilized the phenolate anion in the dark state (6, 13). The chemical and crystallographic studies so far have not identified the stage in the photocycle at which chromophore isomerization occurs, probed earlier structural changes in the photocycle, or indicated how the [pB] state is generated. These ultrafast structural changes in PYP that ultimately lead to the formation of the [pB] state are critical to its function as a photoreceptor.

The recent development of nanosecond time-resolved x-ray crystallography (14, 15) provides the opportunity to study the processes leading to the formation of the [pB] state in crystals of PYP (16) and, hence, to characterize early structural intermediates. The experiments were conducted at the white beamline ID-9 at the European Synchrotron Radiation Facility (ESRF), Grenoble, France, in a manner closely similar to that used to study ligand photolysis, rebinding, and protein relaxation in carbonmonoxy myoglobin (14, 15). The photocycle was initiated by delivery of a focused, unpolarized,

Elaborate systems exist in a wide variety of species to gather light energy and convert it into chemical energy or into a structural signal that ultimately leads to a biological response. The structural bases for these conversions are not well understood. The initial chemical step associated with photoactivity is often photoisomerization of a highly conjugated protein prosthetic group that may generate an altered signaling conformation. This is subsequently recognized by a diffusible or other messenger that delivers the signal to downstream effectors (1). The best studied example is the generation of the

meta II state of mammalian sensory rhodopsin by photoisomerization of its opsin chromophore and the subsequent activation of several molecules of transducin during the long half-life of the meta II intermediate (2). We describe the early structural changes that occur upon absorption of light in a member of a particularly simple class of bacterial photoreceptors: the xanthopsins (3).

The xanthopsin from the photoautotrophic purple eubacterium *Ectothiorhodospira halophila*, known as photoactive yellow protein (PYP), is a small, 14-kD, water-soluble protein in which a 4-hydroxy cinnamic acid chromophore is covalently linked through a thioester to the  $\gamma$  sulfur of Cys<sup>69</sup> (4). PYP appears to serve as the initial response generator in *E. halophila* for a light-initiated signaling cascade that leads ultimately to a negative phototactic response (5). The biochemical and genetic details of this signal transduction process are, at present, unknown.

The chromophore is stabilized in the *trans* configuration as the phenolate anion in the binding pocket of the dark-state protein, denoted pG (Figs. 1 and 2A). The chro-

B. Perman, Department of Biochemistry and Molecular Biology, University of Chicago, Chicago, IL 60637, USA. V. Šrajer, Z. Ren, T.-y. Teng, C. Pradervand, K. Moffat, Department of Biochemistry and Molecular Biology and the Consortium for Advanced Radiation Sources, University of Chicago, Chicago, IL 60637, USA.

T. Ursby, Molecular Biophysics, Chemical Center, Lund University, Post Office Box 124, S-221 00 Lund, Sweden. D. Bourgeois, F. Schotte, M. Wulff, European Synchrotron Radiation Facility, 38043 Grenoble Cedex, France. R. Kort and K. Hellingwerf, Laboratory for Microbiology, E. C. Slater Institute, 1018 WS Amsterdam, Netherlands.

\*To whom correspondence should be addressed. E-mail: moffat@cars.uchicago.edu